
Regression with Conditional GAN

Karan Aggarwal*
University of Minnesota
aggar081@umn.edu

Matthieu Kirchmeyer
Criteo AI Lab
m.kirchmeyer@criteo.com

Pranjal Yadav
Criteo AI Lab
p.yadav@criteo.com

S. Sathya Keerthi
Criteo AI Lab
s.selvaraj@criteo.com

Patrick Gallinari
Criteo AI Lab
p.gallinari@criteo.com

Abstract

In recent years, impressive progress has been made in the design of implicit probabilistic models via Generative Adversarial Networks (GAN) and its extension, the Conditional GAN (CGAN). Excellent solutions have been demonstrated mostly in image processing applications which involve large, continuous output spaces. There is almost no application of these powerful tools to problems having small dimensional output spaces. Regression problems involving the inductive learning of a map, $y = f(x, z)$, z denoting noise, $f : \mathbb{R}^n \times \mathbb{R}^k \rightarrow \mathbb{R}^m$, with m small (e.g., $m = 1$ or just a few) is one good case in point. The standard approach to solve regression problems is to probabilistically model the output y as the sum of a mean function $m(x)$ and a noise term z ; it is also usual to take the noise to be a Gaussian. These are done for convenience sake so that the likelihood of observed data is expressible in closed form. In the real world, on the other hand, stochasticity of the output is usually caused by missing or noisy input variables. Such a real world situation is best represented using an implicit model in which an extra noise vector, z is included with x as input. CGAN is naturally suited to design such implicit models. This paper makes the first step in this direction. Through several artificial and real world datasets, we demonstrate CGAN to be an effective approach for solving regression problems. We compare against Gaussian Processes and show that CGAN has excellent output likelihood properties and possesses the ability to model complex noise forms in a better way.

1 Introduction

Regression is an important problem in statistics and machine learning [4]. In regression, the true output ($y \in \mathbb{R}^m$) is a continuous and stochastic function of the input ($x \in \mathbb{R}^n$):

$$y = f(x, z) \text{ where } z \in \mathbb{R}^k \text{ is the noise vector.} \quad (1)$$

Regression methods attempt to model f by induction using a training data of many (x, y) pairs collected from the real world. Most of these methods [4] model the noise in an additive manner, *i.e.*,

$$y = \hat{f}(x) + z \quad (2)$$

where z is an additive unimodal noise with parameters; for example, $z \sim \mathcal{N}(0, \Sigma)$, the zero-mean Gaussian with covariance matrix Σ . This is usually done for convenience, to write a closed form expression for the conditional density, $p(y|x)$. Regression using Gaussian processes (GPs) [17] is a great example of a state-of-the-art regression method that uses this additive noise modeling.

*Work was done during author's internship at Criteo AI Lab, Palo Alto, CA

There are also some extended types of additive noise modeling: heteroscedastic regression, in which the noise z in (2) is chosen as a function of x ; regression with multi-modal posteriors, where $p(y|x)$ is a multi-modal distribution, etc. Typically, a separate set of methods is developed for each such type of modeling, for example, the extended GP method in [11].

All the above mentioned models are special cases of (1). Also, in real world systems, how noise enters the true y -generation process is generally unknown, and so, ideally it is best to leave it to a non-parametric method to form f . For instance, in many situations, stochasticity of y arises because several input variables are unknown and that affect y jointly in a non-linear fashion together with the known variables; in general, the dimensionality of the set of unknown variables is also not known.

Thus, a direct modeling of (1) can be very worthwhile. Let's make the assumption that z is a known distribution, e.g., Gaussian². Still, the difficulty is that (1) is an implicit probabilistic model and hence, forming and working with the density function, $p(y|x)$ is hard. In recent years, impressive progress has been made in Conditional Generative Adversarial Networks (CGAN) [13] precisely to handle this difficulty. CGAN uses an auxiliary non-parametric function (e.g., DNN) to model the loss function (e.g., Jensen-Shannon or KL divergence) between the implicit probabilistic output model in (1) and the true $p(y|x)$ represented by the training samples.

However, CGAN has been mainly applied to domains such as images [1] where m , the dimension of y is large (several thousands) and the noise dimension, k is much smaller (ten to twenty). Little effort³ has been made to explore the use of CGAN for solving regression problems where k is typically equal or larger than m . This paper aims to fill this gap. We choose several synthetic and real world datasets from the various types of regression problem domains (Sections 3-6). We implement a basic CGAN set up (Section 2) without any extensive tuning of hyperparameters. We take a basic GP setup with tuned hyperparameters (Section 2) as the baseline method to compare and evaluate CGAN. We conduct experiments to demonstrate that CGAN is easily competitive with the basic GP. This should not be taken as a serious benchmarking against the best possible regression methods. The aim is only to point out that CGAN can be a powerful tool for solving regression problems and so it is worthy of further focused research for application to real world regression problems.

2 Experimental Setup and Implementation

We use the standard CGAN [13] formulation in which the discriminator network corresponds to minimizing the Jensen-Shannon divergence between the true and modeled $p(y|x)$ distributions. Alternatively, one could use Wasserstein GAN [2], MMD GAN [12], or f-GAN ideas for minimizing KL divergence [14]. Note that each of these models optimizes a different loss function, which could impact the performance. We use a GP with RBF kernel [17] as the baseline to compare CGAN against.

2.1 Metrics

We report two metrics with each experiment: Negative Log Predictive Density (NLPD) and Mean Absolute Error (MAE). NLPD is taken as the main metric of interest since, for many real world regression problems, studying the goodness of the estimate of uncertainty is of great interest.

NLPD computed using Parzen windows Since CGAN models $p(y|x)$ implicitly, it can only generate samples of y for each given x . In the GAN literature, Parzen windows has been used [3, 9] to approximate $p(y|x)$ using such samples and then use it for evaluating NLPD; we do the same in this paper. We generate 100 samples of y for each x to build the Parzen windows distribution. Please note that probability density can take unlimited positive values, and hence, NLPD can be negative.

MAE Given a test dataset, $\{(x_i, y_i)\}_{i=1}^N$, MAE for a regressor f is defined as $\frac{1}{N} \sum_{i=1}^N |y_i - \hat{y}_i|$ where \hat{y}_i is a single central value returned by the regressor at $x = x_i$. For regressors that generate a distribution $p(y|x_i)$, we define \hat{y}_i to be the median of $p(y|x_i)$; note that median is the central estimate that minimizes mean absolute error. For GP, $p(y|x_i)$ is a Gaussian, and so \hat{y}_i is taken to be the mean

²This is reasonable since complex distributions can be formed by nonlinear transformation of a Gaussian.

³Chapfuwa et al. [5] is a special use of CGAN with survival analysis for time-to-event modeling.

of $p(y|x_i)$ as returned by the model. For CGAN, we generate a sample of 100 y values for the given x_i and take the median of the sample points to be \hat{y}_i .

Confidence and uncertainty when reporting metrics Given the underlying uncertainty in the evaluation of the CGAN method (dependent on the sample drawn from $p(y|x)$), we report the mean over 10 evaluation runs. We found the standard deviation of the metrics over these different samples to be small relative to the mean values ($< 10^{-3}$). In later sections, when we report metrics, they are mean values from 10 runs; also, when we mention a value in **bold**, it will mean that the method whose metric is reported in bold is statistically significantly better than the other model on that metric.

2.2 Experimental setup

Datasets We use two types of datasets: synthetic and real world. We generate four datasets with increasing complexity in noise and the nature of the f function in (1). Description of these datasets and the results on them are given in sections 3- 5. We used two real world datasets (see section 6 for results) - California housing (CA-housing) and Ailerons (aileron)⁴.

Preprocessing A different preprocessing strategy was used on synthetic data and real world data. On real world experiments, input features were scaled to have zero mean and unit variance. On ailerons, we scale y by 1000. On the synthetic datasets, we do not scale features as they already have a reasonably normalized range of inputs and outputs.

Models We use Keras [6] and GPy [10] libraries for experiments. CGAN related code was derived from <https://github.com/eriklindernoren/Keras-GAN>. For GP, we use the GPy package which provides a GP code with automatic hyperparameter optimization.

Dataset statistics We split our datasets into train, validation, and test sets. On synthetic datasets, each set is taken to be of size 1000. On real world datasets we generate the validation set by splitting the training set. For CA-housing, our training, validation, and test sets have a size of 11610, 3870 and 5160, respectively. For ailerons we split the data to 7154 training and 1649 validation samples. ailerons provides an explicit test set of 4947 samples on which we report our results.

Hyperparameter tuning Hyperparameter tuning was done using the validation set. Hyperparameters were tuned to minimize NLPD since that is our main metric of interest. For GP we chose the RBF kernel; this amounts to tuning three hyperparameters: length, variance of the kernel, and standard deviation of the Gaussian noise. These were tuned for each experiment using GPy that provides automated tuning of hyperparameters.

We use DNN for CGAN. Following are the details of CGAN architecture used in our experiments. We use one base architecture for all our experiments. The *Generator* uses a six layered network. We separately feed input x and noise z through a three-layered MLP and concatenate the output representations to a three-layered network. Except for the final layer that employs linear activation, we use exponential linear unit (ELU) [7] as activation function. Addition of a direct connection from z to the final linear unit can help model additive noise but was not necessary. We generally found ELU to work better than activations such as ReLU, leaky-ReLU, or tanh. The *Discriminator* uses a four-layered network. It feeds inputs x and y through a single non-linear layer, and then passes the concatenated outputs through a three-layered MLP whose final layer uses sigmoid activation.

The above architecture worked well on synthetic datasets. The following choice of number of neurons per layer worked well in general: 40 neurons for complex noise datasets (heteroscedastic, exp, and multi-modal) and 15 for simple additive noise datasets (linear and sinus). For real world datasets we increase the number of layers and neurons. For CA-housing and ailerons we use a seven-layered network, with one layer of size 100 for x and noise z , whose outputs are concatenated and passed on to another set of six-layers of size 50.

We use the Adam optimizer and tune it with learning rates of $\{10^{-2}, 10^{-3}, 10^{-4}\}$. We found the learning rates of 10^{-4} for generator and 10^{-3} for discriminator works uniformly well. Improvements are possible with a decay of 10^{-3} on generator’s learning rate.

⁴Taken from <http://www.dcc.fc.up.pt/~ltorgo/Regression/DataSets.html>

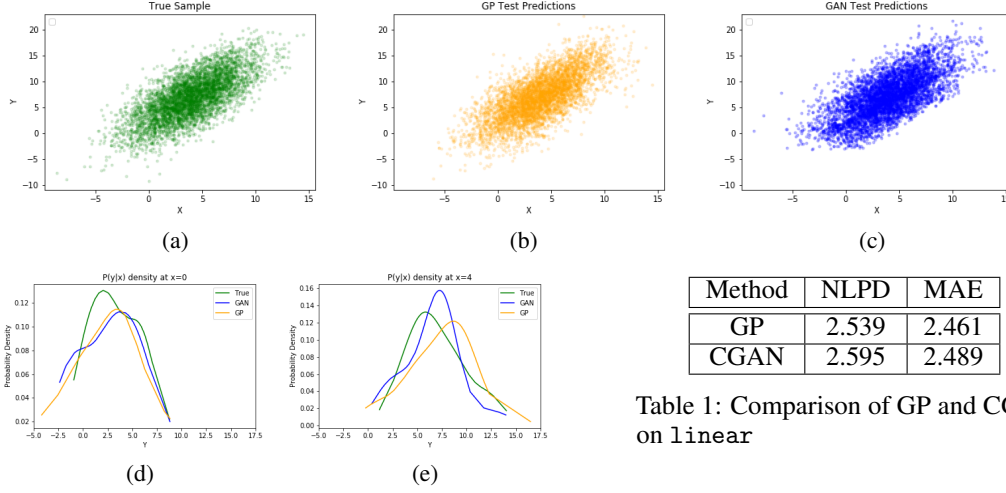


Table 1: Comparison of GP and CGAN on linear

Figure 1: linear dataset. y samples generated by: (a) True model, (b) GP predictions, and (c) CGAN predictions for various x test values. Subplots (d) and (e) show the three probability densities $p(y|x)$ at $x = 0$ and $x = 4$.

The number of epochs was fixed to 2000 on synthetic experiments and 500 on real world datasets. The ratio of training steps of the discriminator over that of the generator was set to 1. Loss curves are stable and converge to the cross entropy of a random discriminator prediction. Batch size of 100 was used in our experiments. The dimension of the noise z was fixed to one on all experiments (including synthetic and real-world). We increase this dimension in the studies of Section 5 and 6 to analyze the effect of higher dimensional noise. Experiments were run on a machine with 16GB RAM and 2.7 GHz processor speed. No significant speedup was noticed when using a Tesla M40 24GB GPU card.

Visualization of experimental results We take key x values and plot the conditional probability density using a Gaussian kernel density estimator. On these plots, we sample 200 times $p(y|x_i)$ for each method (CGAN or GP) at each x_i . Due to this, on some plots we may not see perfect Gaussian distributions for GP. To further investigate distributions being generated (predicted) by these methods, we plot generated samples from CGAN and GP.

3 Additive noise

We first consider the regression scenario with additive noise, $y = f(x) + z$ which is a common assumption made by most regression models. We take z to be Gaussian noise. Commonly used regression models such as GPs are expected to perform well on it, since they model additive Gaussian noise explicitly. This is a basic test for CGAN, which should also be able to model Gaussian noise easily, though the design happens via implicit modeling.

3.1 Gaussian noise dataset (linear)

We first generate a dataset with standard Gaussian noise with $y = x + z$, where $x \sim \mathcal{N}(4, 3)$ and $z \sim \mathcal{N}(3, 3)$. Figure 1 shows the generated samples of the true model, GP and CGAN. Clearly, the sample cloud produced by GP looks more similar to the true samples compared to CGAN. Figure 1 also lists NLPD and MAE metric values for the two methods on test data. There is not a significant difference between the two methods in terms of NLPD and MAE metrics. Since here $f(x) = x$ is quite simple, we next try a complex f to see if CGAN is capable of modeling simple noise with a bit more complex f .

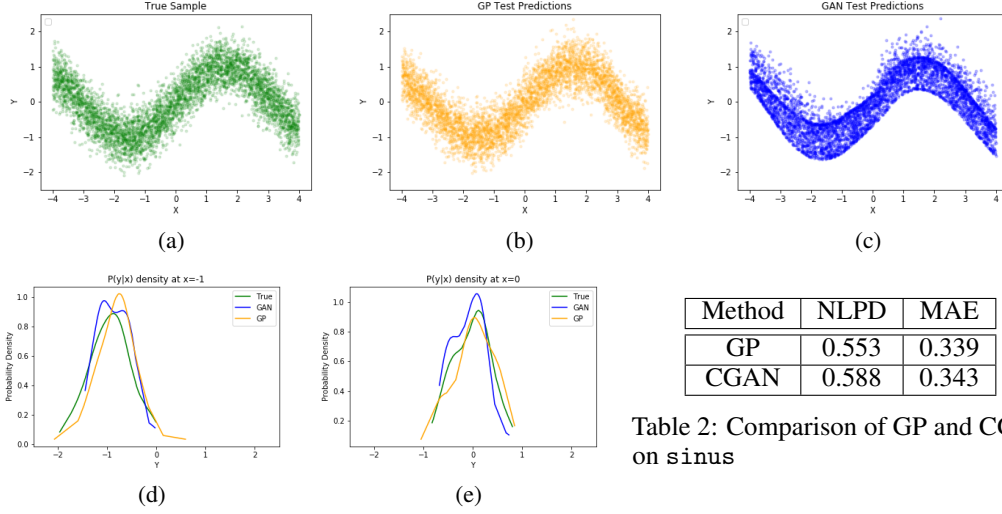


Table 2: Comparison of GP and CGAN on sinus

Figure 2: sinus dataset. y samples generated by: (a) True model, (b) GP predictions, and (c) CGAN predictions for various x test values. Subplots (d) and (e) show the three probability densities $p(y|x)$ at $x = -1$ and $x = 0$.

3.2 Sinusoidal dataset (sinus)

We use Gaussian noise but use $y = \sin(x) + z$ to generate a more complex function of x , where $z \sim \mathcal{N}(0, 1)$, $x \sim \mathcal{U}[-4, 4]$ and \mathcal{U} is the uniform distribution. This is again a simple problem for non-linear regression models like GP. Figure 2 shows samples generated by these methods and the true function. Here too, GP clearly produces more realistic samples than CGAN. The figure also gives the NLPD and MAE metric values on the test data, with CGAN's performance being a tad lower. This case also shows that CGAN is capable of modeling complex functional relationships between inputs and outputs with a simple linear additive noise form. Even with additive noise form,

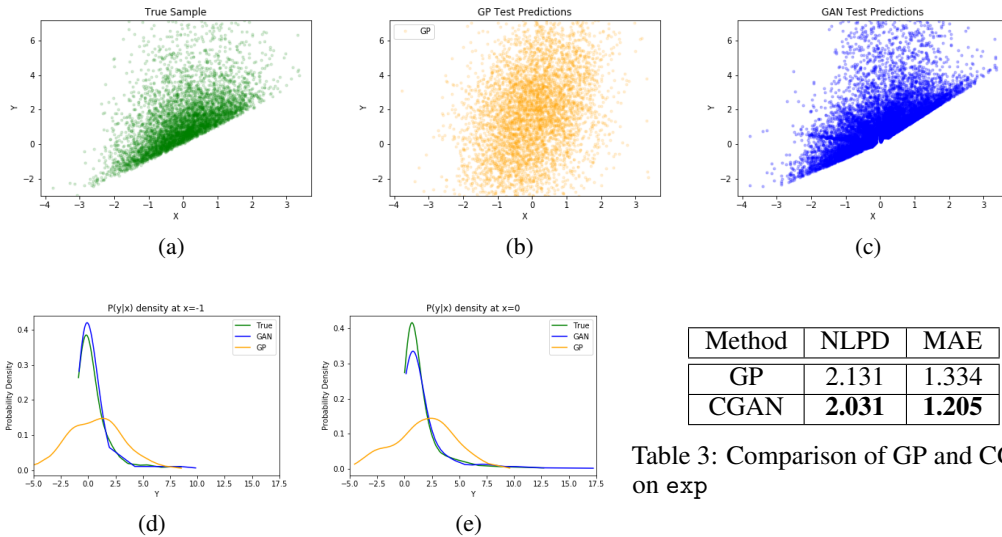


Table 3: Comparison of GP and CGAN on exp

Figure 3: exp dataset. y samples generated by: (a) True model, (b) GP predictions, and (c) CGAN predictions for various x test values. Subplots (d) and (e) show the three probability densities $p(y|x)$ at $x = -1$ and $x = 0$.

CGAN has an advantage over GP when the noise is unimodal but exhibits asymmetric tails, *e.g.*, exponential noise. We investigate exponential noise next.

3.3 Exponential noise dataset (exp)

We use the following generation process to generate exponential noise case: $y = x + \exp(z)$ where $x, z \sim \mathcal{N}(0, 1)$. From Figure 3 we see that CGAN captures asymmetry while GP assumes normal noise (symmetric); this results in better NLPD values for CGAN. This demonstrates CGAN’s modeling capacity to generate asymmetric tailed noise unlike GP that assumes a symmetric distribution. We need to use special GP models like warped GPs to overcome this issue [16], while we use the same GAN architecture we used in previous two sections with minimal modification (larger layer size). The natural next step is to investigate with non-additive complex noise forms, ones which are generally encountered in real world.

4 Heteroscedastic noise dataset (heteroscedastic)

The previous datasets use an additive noise form that is independent of x . However, real world phenomena exhibit more complex noise. We generate a dataset with heteroscedastic noise, *i.e.*, noise that is dependent on x . We use the following generation process: $y = x + h(x, z)$ where $h(x, z) = (0.001 + 0.5|x|) \times z$ and $z \sim \mathcal{N}(1, 1)$. The interesting region of this dataset is around $x = 0$; in this region noise is small compared to other regions of input x . Figure 4 shows the samples generated by these methods and the true sample distribution. CGAN generates more realistic samples compared to GP that fails to capture the heteroscedastic noise structure. CGAN also has much better NLPD values as shown in Table 3. While using heteroscedastic GPs [17] would also make GPs do better on this dataset, the important point to note here is that, though the CGAN architecture used is similar to the experiments of Section 3.1, CGAN has easily learnt to model a very different type of noise. This demonstrates the capability of CGAN in modeling complex noise forms.

5 Beyond regression: multi-modal posteriors (multi-modal)

Next, we take a case in which the interaction between noise and x is more complex. We construct a simple dataset with a multi-modal $p(y|x)$ distribution which also changes with x , to examine whether CGAN can capture such complex distributions. Clearly, GPs are disadvantaged on this task. Such

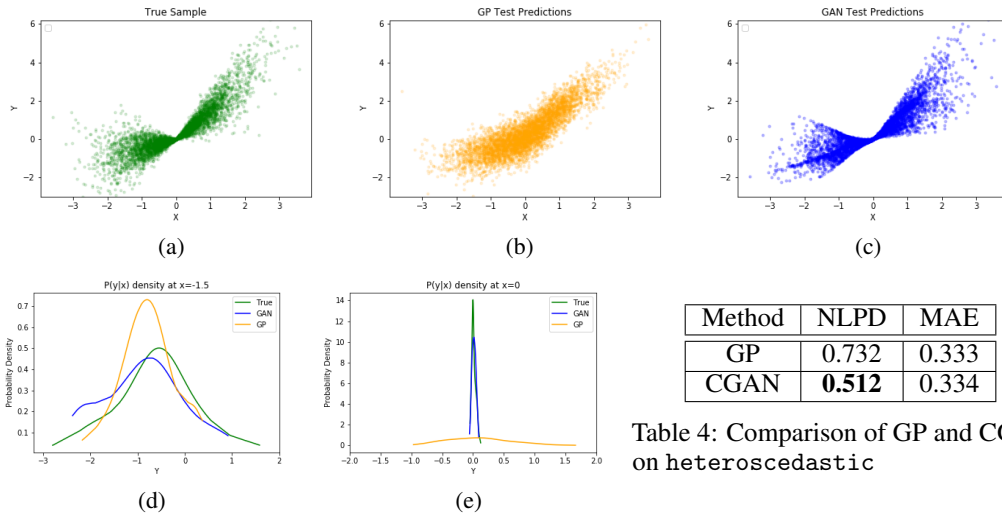


Table 4: Comparison of GP and CGAN on heteroscedastic

Figure 4: heteroscedastic dataset. y samples generated by: (a) True model, (b) GP predictions, and (c) CGAN predictions for various x test values. Subplots (d) and (e) show the three probability densities $p(y|x)$ at $x = -1.5$ and $x = 0$.

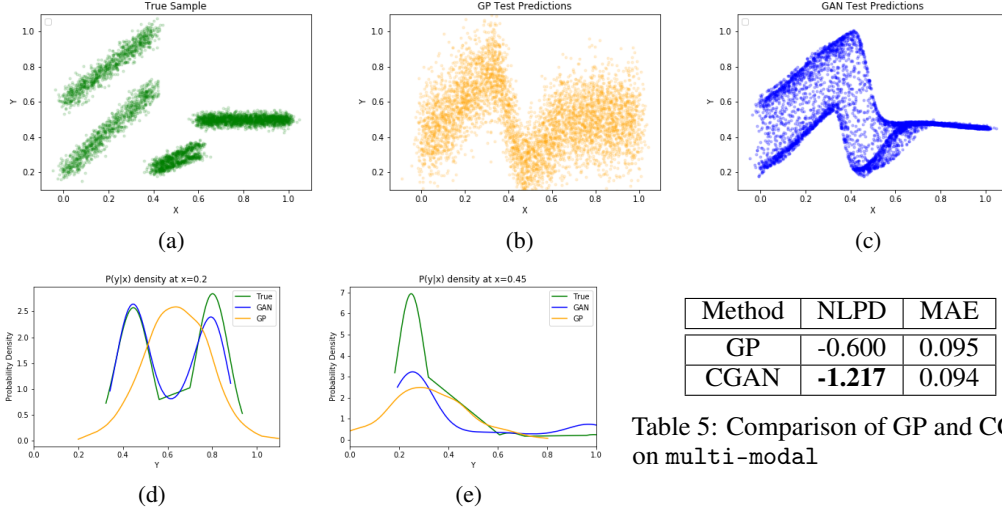


Table 5: Comparison of GP and CGAN on multi-modal

Figure 5: multi-modal dataset. y samples generated by: (a) True model, (b) GP predictions, and (c) CGAN predictions for various x test values. Subplots (d) and (e) show the three probability densities $p(y|x)$ at $x = 0.2$ and $x = 0.45$.

distributions can occur in real world phenomena such as certain dynamical systems which switch between multiple states [8], depending on latent factors like temperature; this can create scenarios where the same input x can be mapped to two values of y . Few models exist in the literature for multi-modal regression [8].

We use the following procedure to generate a multi-modal data where y is: $1.2x + 0.03z$ or $x + 0.6 + 0.03z$ when $0.4 < x$; $0.5x + 0.01z$ or $0.6x + 0.01z$ when $0.4 \leq x < 0.6$ and; $0.5 + 0.02z$ when $0.6 \leq x$, with $z \sim \mathcal{N}(0, 1)$ and $x \sim \mathcal{U}[0, 1]$.

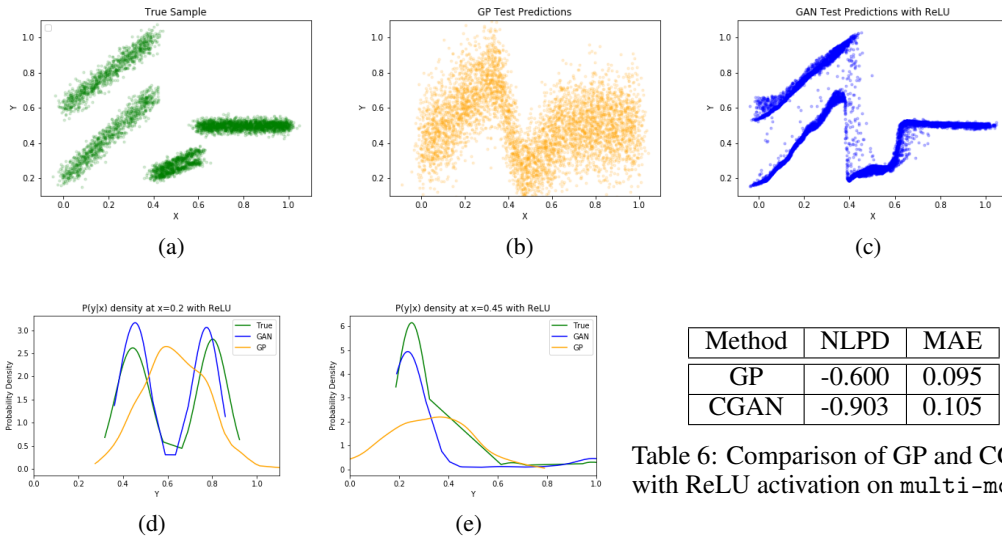


Table 6: Comparison of GP and CGAN with ReLU activation on multi-modal

Figure 6: multi-modal dataset using ReLU activation for CGAN. y samples generated by: (a) True model, (b) GP predictions, and (c) CGAN predictions for various x test values. Subplots (d) and (e) show the three probability densities $p(y|x)$ at $x = 0.2$ and $x = 0.45$.

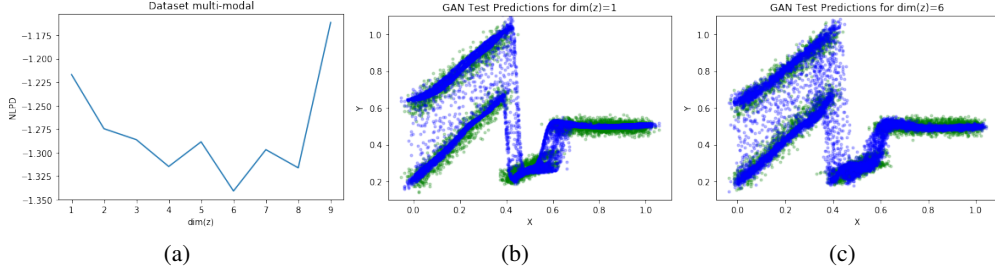


Figure 7: Study on input noise dimension $\dim(z)$: (a) shows variation of NLPD with $\dim(z)$ for multi-modal; (b) shows the output prediction of CGAN (blue) for $\dim(z) = 1$ while (c) shows the output predictions of CGAN (blue) for the best dimension value found in $[1, 10]$, i.e., $\dim(z) = 6$ overlaid on true distribution (green). 2 samples were used for each x .

Figure 5 shows the generated test samples and samples predicted by GP and CGAN. CGAN clearly displays a remarkable ability to model the multi-modal nature of the underlying data, while GP expectedly fails to do so since GP can only generate a (unimodal) Gaussian distribution for a given x . This also results in poor performance of GP in $x \geq 0.6$ region since it struggles to match the noise across different regions. Few models exist in the literature for multi-modal regression and it is encouraging to see that CGAN can model it implicitly. This demonstrates the versatility of CGAN to capture complex conditional distributions, while other regression methods require special modifications for the same.

It is interesting to note that the ELU activation function smoothens the overall shape of the generated y distribution. ELU produces a smoothing over distribution of y when there are discontinuities in y over x . Applying sparser activations such as ReLU can help reduce the smoothness. See Figure 6 (a) for the discontinuity at $x = 0.4$ and $x = 0.6$.

We perform an experiment to replace ELU with ReLU activation function. Figure 6 (c) shows the generated samples by this ReLU network. From visual inspection we can see that ReLUs are able to account for these discontinuities better compared to samples obtained via ELU. However, ReLU struggles with forming the noise levels and shapes on the dominant clusters compared to ELU; we also notice that using ReLU leads to higher variance in practise with a lower mean value than a network with ELU activation.

Increasing the dimensionality of noise To study the effect of dimensionality of noise on CGAN performance, we vary $k = \dim(z)$ over $\{1, 2, 3, 4, 5, 6, 7, 8, 9\}$. Figure 7(a) shows NLPD values as we increase the dimensionality of noise. We get the lowest value of $\text{NLPD} = -1.34$ at $k = 6$. To point out the goodness of this choice of $\dim(z)$, we show the CGAN prediction samples generated at $\dim(z) = 1$ and $\dim(z) = 6$ in Figure 7. There is an improvement in faithfulness to the true distribution density when noise dimensionality is set correctly. These results imply that, for problems with complex noise, using a higher dimensional noise can help obtain improved performance.

6 Real world Datasets

We run experiments on two real world datasets: California housing and Ailerons.

California housing (CA-housing) The task here is to predict the price of a property in California given property attributes. The dataset contains eight input attributes such as location, size, and number of rooms in the property.

Table 7: Comparison of GP and CGAN on Real World datasets

	ailerons		CA-housing (full)		CA-housing (1 input)	
Method	NLPD	MAE	NLPD	MAE	NLPD	MAE
GP	0.410	0.159	0.830	0.383	1.238	0.615
CGAN	-0.255	0.128	0.681	0.364	1.165	0.624

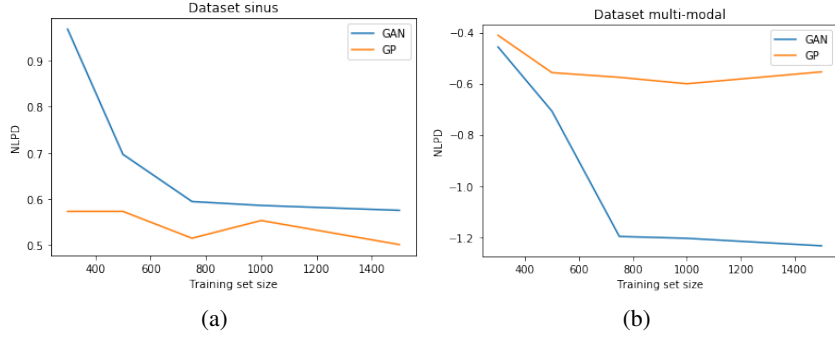


Figure 8: The effect of the size of training data for a) sinus b) multi-modal.

Ailerons (aileron) The inputs here describe the status of F16 aeroplane, with the goal to predict the control action on the aircraft’s ailerons. The status of the aeroplane is described by 40 continuous inputs like climb rate, pitch, and curl of the aeroplane’s trajectory.

Table 7 depicts the results from these two datasets. CGAN provides better NLPD as well as MAE compared to GP. This is in line with the results observed in earlier sections on some synthetic datasets. This could probably be explained by the noise in these datasets being non-additive. As pointed out earlier in subsection 2.2, we had to use more complex architectures on these real world datasets to get better results to cater to higher dimensional input space.

Introducing noise by removing input features In real world scenarios, it may not be possible to observe all the input variables x that lead to the observed outcome y . In such cases, the unknown input variables represent the noise. CGAN can model such a scenario naturally with z representing the unknown variables. To show the value of CGAN in such a scenario, we remove several inputs from the CA-housing dataset. We run XGBoost [18] to obtain feature importance values on CA-housing. The feature, *longitude*, accounts for 62% of the total feature importance; we take this single feature as the only known feature in our experiment, and use noise of dimension $\dim(z) = 8$ to account for the removed inputs. Results on this modified dataset are reported under CA-housing (1 input) column in Table 7. Interestingly, GP is competitive with CGAN using this single feature.

7 Effect of training size

GP, like other Bayesian methods, is known to perform well with small datasets. This is because these methods average the predictions using the posterior in the weight space. CGAN does not enjoy this property since it uses only a single set of weights. Given this, it is worthwhile to investigate how CGAN behaves compared to GP when the training sample size becomes small. We report the results in Figure 8 on sinus and multi-modal as the training size N decreases. Here we take N to be in $\{300, 500, 750, 1000, 1500\}$. We notice that the performance of GP is stable over the range of training set sizes. CGAN suffers from a reduced training set size. Interestingly, on the multi-modal dataset we find that below 300 instances, GP is performing as well as CGAN.

8 Conclusion

We have demonstrated that CGAN can be attractive for solving regression problems. The main advantages of CGAN are: it models noise more naturally; and, it can handle different types of regression models in one formulation and implementation. Also, compared to CGAN for large structured domains such as images, it is much simpler to set up and design because: (a) it does not need any expert level setting up of the generating function, f ; (b) the noise dimension, k can be chosen to be equal or higher than m , the dimension of the output, y , and so, "zero" gradient issues are easily avoided; and, (c) since regression problems have either one or at most a few modes in y for a given x , "missed modes" or "mode collapse" issues are less of an issue.

CGAN is worthy of further exploration for solving regression problems. In this paper we only experimented with datasets with one dimensional output, $m = \dim(y) = 1$. It would be useful to evaluate CGAN on datasets with multiple, nonlinearly correlated outputs. Problems in joint, multi-time-series prediction, for example, those arising in applications such as financial and weather forecasting that involve many unknown variables, can gain a lot from the application of CGAN. There are also many generic directions for future work. In this paper, we employed the standard CGAN discriminator that corresponds to minimizing the Jensen-Shannon divergence. Since maximum likelihood corresponds to minimizing KL divergence, f-GAN ideas in [14] can be used to change the discriminator suitably, and this could result in better NLPD generalization. Detailed hyperparameter tuning needs to be explored. Design of scalable CGAN implementations suited for regression is another key direction. Designing Bayesian version of CGAN [15] would give great gains on small training datasets. With these leading to much better performing CGAN implementations, we can return to do a more thorough benchmarking of CGAN against the current best regression solvers.

References

- [1] Grigory Antipov, Moez Baccouche, and Jean-Luc Dugelay. Face aging with conditional generative adversarial networks. In *2017 IEEE International Conference on Image Processing (ICIP)*, pages 2089–2093. IEEE, 2017.
- [2] Martin Arjovsky, Soumith Chintala, and Léon Bottou. Wasserstein GAN. *arXiv preprint arXiv:1701.07875*, 2017.
- [3] Yoshua Bengio, Grégoire Mesnil, Yann Dauphin, and Salah Rifai. Better mixing via deep representations. In *International conference on machine learning*, pages 552–560, 2013.
- [4] Christopher M Bishop. *Pattern recognition and machine learning*. springer, 2006.
- [5] Paidamoyo Chapfuwa, Chenyang Tao, Chunyuan Li, Courtney Page, Benjamin Goldstein, Lawrence Carin Duke, and Ricardo Henao. Adversarial time-to-event modeling. In *International Conference on Machine Learning*, pages 734–743, 2018.
- [6] François Chollet. keras. <https://github.com/fchollet/keras>, 2015.
- [7] Djork-Arné Clevert, Thomas Unterthiner, and Sepp Hochreiter. Fast and accurate deep network learning by exponential linear units (elus). *arXiv preprint arXiv:1511.07289*, 2015.
- [8] Jochen Einbeck and Gerhard Tutz. Modelling beyond regression functions: an application of multimodal regression to speed–flow data. *Journal of the Royal Statistical Society: Series C (Applied Statistics)*, 55(4):461–475, 2006.
- [9] Ian Goodfellow, Jean Pouget-Abadie, Mehdi Mirza, Bing Xu, David Warde-Farley, Sherjil Ozair, Aaron Courville, and Yoshua Bengio. Generative adversarial nets. In *Advances in neural information processing systems*, pages 2672–2680, 2014.
- [10] GPy. GPy: A gaussian process framework in python. <http://github.com/SheffieldML/GPy>, 2012.
- [11] Quoc V Le, Alex J Smola, and Stéphane Canu. Heteroscedastic gaussian process regression. In *Proceedings of the 22nd international conference on Machine learning*, pages 489–496. ACM, 2005.
- [12] Chun-Liang Li, Wei-Cheng Chang, Yu Cheng, Yiming Yang, and Barnabás Póczos. MMD GAN: Towards deeper understanding of moment matching network. In *Advances in Neural Information Processing Systems*, pages 2203–2213, 2017.
- [13] Mehdi Mirza and Simon Osindero. Conditional generative adversarial nets. *arXiv preprint arXiv:1411.1784*, 2014.
- [14] Sebastian Nowozin, Botond Cseke, and Ryota Tomioka. f-GAN: Training generative neural samplers using variational divergence minimization. In *Advances in neural information processing systems*, pages 271–279, 2016.
- [15] Yunus Saatci and Andrew G Wilson. Bayesian GAN. In *Advances in neural information processing systems*, pages 3622–3631, 2017.
- [16] Edward Snelson, Zoubin Ghahramani, and Carl E Rasmussen. Warped gaussian processes. In *Advances in neural information processing systems*, pages 337–344, 2004.

- [17] Christopher KI Williams and Carl Edward Rasmussen. Gaussian processes for regression. In *Advances in neural information processing systems*, pages 514–520, 1996.
- [18] XGBoost. XGBoost: Scalable and flexible gradient boosting. <https://xgboost.ai/>, 2012.